Bridging the gap: Western rock skinks (Trachylepis sulcata) have a short history in South Africa

Article *in* Molecular Ecology · March 2011

DOI: 10.1111/j.1365-294X.2011.05047.x · Source: PubMed

3 authors:

Daniel M Portik
Pacific Biosciences
78 PUBLICATIONS **1,698** CITATIONS
SEE PROFILE

A. M. Bauer
Villanova University
782 PUBLICATIONS **17,952** CITATIONS
SEE PROFILE

Todd Jackman
Villanova University
154 PUBLICATIONS **6,547** CITATIONS
SEE PROFILE

MOLECULAR ECOLOGY

Molecular Ecology (2011) **20**, 1744–1758 doi: 10.1111/j.1365-294X.2011.05047.x

Bridging the gap: western rock skinks (*Trachylepis sulcata*) have a short history in South Africa

DANIEL M. PORTIK,* AARON M. BAUER and TODD R. JACKMAN

Department of Biology, Villanova University, 800 Lancaster Avenue, Villanova, PA 19085-1699, USA

Abstract

Phylogeographic patterns in wide-ranging species in southern Africa remain largely unexplored, especially in areas north of South Africa. Here, we investigate population structuring, demographic history, and the colonization pattern of the western rock skink (*Trachylepis sulcata*), a rock-dwelling species with a range extending from southwestern South Africa into Angola. Using 1056 bp from the mitochondrial marker *ND2* and > 2.5 kb from three nuclear genes (*EXPH5*, *KIF24*, *RAG-1*), we constructed allele networks, generated extended Bayesian skyline plots and performed population clustering analyses. Analyses of historical demographic patterns show an overall southward range expansion from Northern Namibia into Southern Namibia and South Africa, although we find contrasting genetic breaks across these geographic regions using nuclear and mitochondrial data. We suggest that mtDNA has introgressed across a nuclear break corresponding to the Knersvlakte region of South Africa, a previously proposed biogeographic barrier for rupicolous species. This pattern of mitochondrial variation contrasts sharply to that of other South African taxa previously investigated, which all show significant mtDNA differentiation across the Knersvlakte region. Additionally, while other taxa show divergences dating to the Pliocene, *T. sulcata* appears to be a recent arrival in southern Africa, having crossed this barrier and colonized South Africa in the mid-Pleistocene. The complex phylogeographic history of *T. sulcata* corroborates the intricate patterns of genetic variation found in South African taxa and provides novel insight into historical processes affecting species distributed across Namibia.

Keywords: phylogeography, population genetics—empirical, reptiles, speciation

Received 20 June 2010; revision received 1 February 2011; accepted 2 February 2011

Introduction

Southern Africa is a region with a rich geological and climatic history, and throughout time topographic events and changing climatic conditions have allowed for the existence of a wide range of habitat types (Van Zinderen Bakker & Mercer 1986; Lancaster 1989; Coetzee 1993). These changing habitats, coupled with the emergence of biogeographic barriers, have undoubtedly sculpted the current distributions of evolutionary lineages in southern Africa. Compared to North America, Europe and Australia, relatively few phylogeographic studies have been conducted on the herpetofauna in this region (Beheregaray 2008). Reptilian taxa that have been studied in a phylogeographic context include the angulate tortoise (*Chersina angulata*) (Lesia *et al.* 2003; Daniels *et al.* 2007), the speckled padloper (*Homopus signatus*) (Daniels *et al.* 2010), cordylid lizards (Daniels *et al.* 2004), dwarf chameleons (*Bradypodion*) (Tolley *et al.* 2004, 2006, 2008), the rock agama (*Agama atra*) (Matthee & Flemming 2002; Swart *et al.* 2009) and sand lizards (genus *Pedioplanis*) (Makokha 2006; Makokha *et al.* 2007). Geographic structuring of populations has been found in the taxa studied, although most of these studies are based in southwestern South Africa. In particular, the Cape Floristic Region (CFR), an area of high endemism (Cowling *et al.* 2009; Van der Niet & Johnson

Correspondence: Daniel M. Portik, Fax: 510 643 8238;
E-mail: daniel.portik@berkeley.edu
*Present address: Museum of Vertebrate Zoology and Department of Integrative Biology, 3101 Valley Life Sciences Building, University of California, Berkeley, CA 94720-3160, USA.

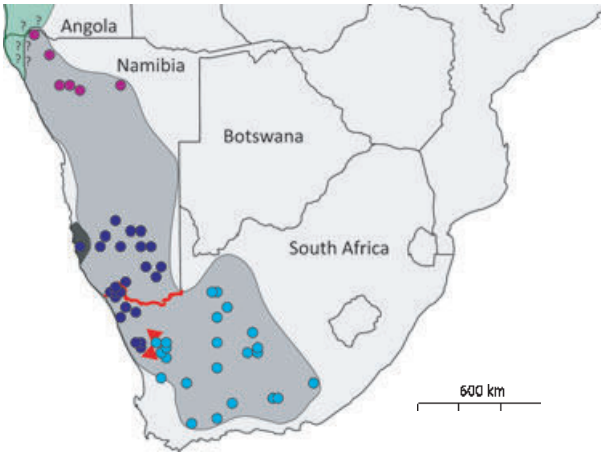

Fig. 1 A map of southern Africa depicting the known range of *Trachylepis sulcata* (based on Branch (1998)). The range of each subspecies is also depicted: *T. s. sulcata* (dark grey), *T. s. ansorgii* (green) and *T. s. nigra* (black). Circles represent sampling localities in three different geographic locations: purple, Northern (Northern Namibia); dark blue, Central (Southern Namibia and Northern Cape west of Knersvlakte region); and light blue, Southern (Northern Cape east of Knersvlakte, Western Cape, Eastern Cape). Two previously proposed biogeographic barriers are highlighted in red, the Orange River (South African–Namib border) and the Knersvlakte region (hourglass shape).

2009; Verboom *et al.* 2009a,b), has been sampled extensively. Comparative phylogeography in the CFR has revealed the impact of rainfall zones and vegetation on the genetic structuring of lizards present in this region (Chase & Meadows 2007; Tolley *et al.* 2009). However, little is known about the geographic and genetic structure of lizards in areas north of South Africa.

Trachylepis sulcata is a broadly distributed, sexually dimorphic, rupicolous skink species with a range extending from the southwestern region of South Africa to Angola (Fig. 1) (Branch 1998). This species inhabits karroid veld, desert and arid savannah habitats found in this region (Branch & Bauer 1995; Bauer & Branch 2001). In addition to the nominate form, two subspecies have been recognized within *T. sulcata* (e.g., Branch 1998). *Trachylepis sulcata ansorgii* (Boulenger 1907) was described from southern Angola, and its status remains uncertain. It was considered valid by Laurent (1964) and Mertens (1971) identified some Namibian specimens as intergrades between *T. s. ansorgii* and *T. s. sulcata*. At least some material from west of the Great Escarpment in northwestern Namibia exhibits the bright throat and infralabial coloration that is supposedly diagnostic of this form, but there appear to be no fixed scalation differences with respect to *T. s. sulcata* (Bauer *et al.* 1993). The other subspecies, *T. s. nigra* (Werner 1915), from the Lüderitz area of coastal Namibia, has also been regarded as valid by some authors (e.g., Mertens 1955), but our research suggests that this melanistic form is not genetically distinct (Portik *et al.* 2010). We do not address the validity of *T. s. ansorgii* herein, but we have included samples previously assigned to *T. s. nigra* in our analysis.

The rupicolous nature of this species may have significant implications for genetic structuring, as fragmentation events and biogeographic barriers are more likely to affect substrate-dependent species. The Orange River and the Knersvlakte region have been previously proposed as potential biogeographic barriers in southern Africa (Fig. 1). The Orange River flows along the South African–Namib border and is associated with a mitochondrial break in the rock agamid, *A. atra* (Matthee & Flemming 2002); however, it is ineffective as a barrier for many other lizard species (Bauer 1999). The Knersvlakte is a large arid plain located in Namaqualand in the northern Western Cape and sits between the Bokkeveld Mountains and the Kamiesberg Mountains. This pebble-covered, sparsely vegetated region is largely unsuitable habitat for rock-dwelling species and appears to be a major biogeographic barrier at the population level for many rupicolous species, including the rock agamid (Matthee & Flemming 2002), the speckled padloper (Daniels *et al.* 2010), the red rock rabbit (*Pronolagus rupestris*) (Matthee & Robinson 1996) and the Cape rock elephant shrew (*Elephantulus edwardii*) (Smit *et al.* 2007). Additionally, speciation patterns in two genera of rupicolous geckos, *Pachydactylus* and *Goggia*, also show major breaks in lineages surrounding the Knersvlakte (Branch *et al.* 1995; Lamb & Bauer 2000). The rock agamid, red rock rabbit and Cape rock elephant shrew display a westward colonization pattern across southern Africa and appear to have crossed the Knersvlakte in this general direction and subsequently expanded northward (Matthee & Robinson 1996; Matthee & Flemming 2002; Smit *et al.* 2007). However, these breaks and patterns were detected using relatively small mitochondrial data sets and remain to be corroborated using nuclear loci.

Given the concordance of genetic breaks in rupicolous taxa across the Knersvlakte, we propose that *T. sulcata* displays similar phylogeographic patterns across this region. As the biogeographic effects of the Orange River are variable, we also examine the efficacy of this geographic feature as a genetic barrier for this particular species. The range of *T. sulcata* allows a novel opportunity to investigate population structuring in a lizard species distributed across Namibia, a country largely unexamined in a phylogeographic context. Using mitochondrial and nuclear data, we examine phylogeographic patterns in *T. sulcata* by employing network analyses, tests for demographic expansion, extended Bayesian skyline plots (EBSPs) and population

clustering analyses. We examine the genetic connectivity of this wide-ranging species and investigate the effects of potential biogeographic barriers on population structure. By combining the historical population size estimates through time with the patterns of phylogeography and population structuring, we infer the colonization pattern of this wide-ranging species and compare this to the patterns found in other previously examined taxa in southern Africa.

Materials and methods

Sampling

We obtained 86 samples representing *Trachylepis sulcata* and a single sample of the closely related species *Trachylepis variegata* (Appendix). Samples of *T. sulcata* were collected from 64 localities ranging from Northern Namibia at the Angolan border to the Eastern Cape in South Africa (Fig. 1). Sampling was widespread throughout the range of *T. sulcata*, except for a gap in central Namibia. Three groupings are defined based on major geographic regions: (i) Northern: Northern Namibia, (ii) Central: Southern Namibia and the Northern Cape (west and north of the Knersvlakte region), and (iii) Southern: the Northern Cape (east of the Knersvlakte region), Western Cape and Eastern Cape (Fig. 1).

DNA extraction and amplification

Whole genomic DNA was extracted from liver or tail samples preserved in 95-100% EtOH. DNA extraction was performed using the Qiagen DNeasy™ tissue kit (Valencia, CA, USA). PCR amplifications were performed with negative controls using forward and reverse primers obtained from published sources (Table 1). Amplifications were conducted in 25-μL volume reactions initiated at 95 °C for 2 min followed by 35 cycles of 95 °C for 35 s, 50 °C for 35 s and 72 °C for 1 min 35 s (with extension increasing 4 s per cycle). Purifications were performed using the Agencourt AMPure PCR purification kit (Agencourt Bioscience, Beverly, MA, USA). Samples were prepared for sequencing using a combination of the BigDye® Terminator v3.1 Cycle Sequencing Kit (Applied Biosystems, Foster City, CA, USA) and CleanSeq (Agencourt Bioscience). Gene products were forward and reverse sequenced using an ABI3700 Automated Sequencer. Sequences were analysed using Geneious v4.6 (Drummond *et al.* 2009) and aligned by eye with no ambiguities.

The complete mitochondrial *ND2* gene with 1056 aligned bases was sequenced. Additionally, partial exonic sequences of *RAG-1* (1149 bases) and two newly developed rapidly evolving orthologous protein-coding nuclear markers, exophilin 5 (*EXPH5*, 941 bases) and kinesin family member 24 (*KIF24*, 554 bases), were sequenced (Portik *et al.* 2010). All sequences are deposited in Genbank (Accession numbers: GU931406–GU931681, HQ829667–HQ829808).

Haplotype estimation

Heterozygous individuals were apparent for all nuclear genes sequenced, and the number of heterozygous sites per individual and total number of heterozygous individuals varied across genes (Fig. 2). The relatively few number of heterozygous sequences in *KIF24* when compared to *RAG-1* and *EXPH5* may be explained by the function of the protein coded by the complete *KIF24* exon (6265 bp in humans). This gene codes for a kinesin-like protein with globular heads containing binding sites for microtubules and ATP, and the 554-bp portion we amplified (starting at human position 1836) may be conserved. The function of exophilin 5 is not well understood, but it may play a role in vesicle trafficking or act as an effector protein for specific Rab family proteins. The functional constraints on this protein are therefore poorly understood. Heterozygous sequences were phased using the program fastPHASE v1.4.0 (Stephens *et al.* 2001; Scheet & Stephens 2006).

Table 1 A list of genes and associated primer sets used in this study

Gene	Primer name	Source	Sequence (5′ to 3′)
RAG-1	RAG1skink F2	Portik *et al.* (2010)	TTCAAAGTGAGATCGCTTGAAA
	RAG1skink R2	Portik *et al.* (2010)	AACATCACAGCTTGATGAATGG
	RAG1skink F370	Portik *et al.* (2010)	GCCAAGGTTTTTAAGATTGACG
	RAG1skink R1200	Portik *et al.* (2010)	CCCTTCTTCTTTCTCAGCAAAA
ND2	MET F1 L4437	Macey *et al.* (1997)	AAGCTTTCGGGCCCATACC
	TRP R3 H5540	Macey *et al.* (1997)	TTTAGGGCTTTGAAGGC
KIF24	KIF24 F1	Portik *et al.* (2010)	SAAACGTRTCTCCMAAACGCATCC
	KIF24 R1	Portik *et al.* (2010)	WGGCTGCTGRAAYTGCTGGTG
EXPH5	EXPH5 F1	Portik *et al.* (2010)	AATAAACTKGCAGCTATGTACAAAACAAGTC
	EXPH5 R1	Portik *et al.* (2010)	AAYCGCCCTTCTGTGAGTGACCTCT

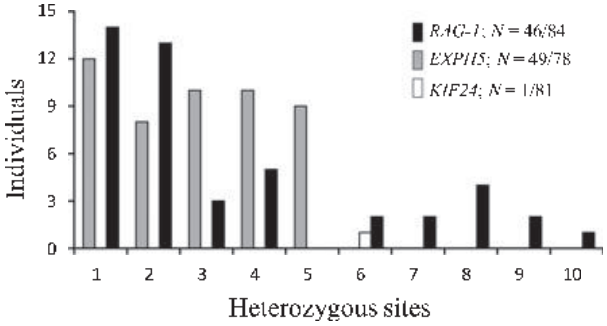

Fig. 2 The frequency of heterozygous individuals for a given number of sites for each nuclear gene analysed. Totals of heterozygous individuals are given along with the total number of individuals sequenced for each gene (N).

Network analyses

Allele networks were constructed for the three nuclear loci analysed (EXPH5, KIF24, RAG-1) using statistical parsimony with a 95% connection significance in the program TCS v1.21 (Clement *et al.* 2000). Analyses were performed using phased nuclear data only, and gaps were treated as a fifth state. The closely related species *Trachylepis variegata* was used to root each nuclear allele network (Portik *et al.* 2010). As a comparison, distance networks for each nuclear gene were also created using the NeighborNet algorithm (Bryant & Moulton 2004) in SplitsTree v4.11.3 (Huson & Bryant 2006). As the statistical parsimony method failed to construct a resolved parsimony network for the mtDNA gene *ND2*, a distance network was created using the NeighborNet algorithm in SplitsTree v4.11.3. Additionally, a multilocus genetic network was constructed by converting allele distance matrices from the three nuclear markers into a standardized distance matrix of individuals using the program POFAD v1.03 (Joly & Bruneau 2006). A distance network was created from the multilocus individual matrix using the NeighborNet algorithm (Bryant & Moulton 2004) in SplitsTree v4.11.3 (Huson & Bryant 2006).

Historical demography and molecular diversity

To obtain estimates of changes in historical population size, extended Bayesian skyline plot (EBSP) were constructed using BEAST v1.5.3 (Drummond *et al.* 2005; Drummond & Rambaut 2007; Heled & Drummond 2008). This method is preferred to Bayesian skyline plots (BSP) because multiple loci are used to estimate effective population size through time. Historical population dynamics estimated using a single locus may be inaccurate because of stochastic processes associated with any given locus, and a multilocus approach provides more accurate estimates of population size (Heled & Drummond 2008). Analyses were conducted separately on the Northern, Central, and Southern regions incorporating both mtDNA and nuclear markers. Substitution models, clock models, and trees were unlinked across all markers; substitution models were chosen using the AIC in jModelTest v0.1.1 (Posada 2008). The mtDNA marker *ND2* was utilized as the stable reference marker to create a reference rate for other markers in the analysis. This gene was chosen because mtDNA evolves more rapidly than nuclear genes and therefore contains more information. A fixed mean substitution rate of 0.47% change per lineage per million years was assigned to the *ND2* gene. This rate was obtained by recalculating the rate obtained by Macey *et al.* (1998) for the agamid genus *Laudakia* by using only their *ND2* data and excluding the *ND1*, *COI* and associated tRNA regions. Substitution rates can vary between lineages; however, phylogenetic work by Townsend *et al.* (2004) based on *ND1*, *ND2*, *COI* and 8 tRNAs illustrates that mtDNA substitution rates between agamids and the genus *Trachylepis* (referred to as *Mabuya*) are comparable. Linear and stepwise models were explored for each population using a strict clock or an uncorrelated log-normal relaxed clock, and runs consisted of 2.5×10^8 generations sampled every 1000 generations. Final models were chosen using Bayes factors, and comparisons are reported as $\log_{10}$ Bayes factors ($\log_{10}$ BF), where a $\log_{10}$ of one implies a model is ten times more likely (Newton *et al.* 1994; Kass & Raftery 1995; Suchard *et al.* 2001). All analyses were examined for stationarity using Tracer v1.5.0 (Rambaut & Drummond 2009).

As a comparison to the extended skyline plots, mismatch distributions, Tajima's *D* and Fu's *Fs* value were calculated for each molecular data set using Arlequin v3.11 (Excoffier & Schneider 2005). For mismatch distribution analysis, the observed distribution of pairwise differences of each gene was compared to data simulated under the sudden expansion model. Multimodal or ragged distributions suggest a historically stable population size, whereas smooth or unimodal distributions imply population expansion (Slatkin & Hudson 1991; Rogers & Harpending 1992). Sum of square deviations and Harpending's raggedness index were used to assess the fit of the data to the model, with significant *P* values allowing rejection of the expansion hypothesis. Tajima's *D* can be used to detect selection or changes in population size, with negative values indicating population expansion or positive selection, and positive values indicating population contraction or balancing selection (Tajima 1989). Fu's *Fs* value is useful for detecting population growth or genetic hitchhiking (Fu 1997). In both tests, populations that have been stable are expected to have values near zero. Further tests of selection were

conducted using the McDonald–Kreitman test (MK; McDonald and Kreitman 1991), which compares synonymous and nonsynonymous substitution rates across different species or populations. MK tests were carried out using DnaSP v5.10.01 (Librado & Rozas 2009).

A hierarchical analysis of molecular variance (AMOVA) was implemented to assess nuclear and mitochondrial sequence variation within populations, between populations and between groups of populations (Excoffier *et al.* 1992). Localities were treated as populations and two-group and three-group designs were implemented. In the two-group design, the Central localities were combined with either the Northern or Southern localities, whereas the three-group design treated the Northern, Central, and Southern localities as separate groups. Uncorrected pairwise differences were utilized to estimate ϕ-statistics, and 5000 random permutations were performed to assess significance using Arlequin v3.11 (Excoffier & Schneider 2005). Additionally, the nucleotide diversity (π), average number of within-population pairwise differences (k) and pairwise fixation indices (F_{ST}) were also calculated using Arlequin v3.11 (Excoffier & Schneider 2005).

Population clustering

The Bayesian clustering program STRUCTURE v2.3.2 (Pritchard *et al.* 2000) was used to analyse fine-scale structuring based on phased allelic data from the three nuclear genes. Samples with missing data for any of the three genes were excluded from the analysis; the number of samples analysed totalled 76. The final settings employed the linkage model with allele frequencies correlated, contained a burn-in length of 1×10^5 and ran 5×10^5 generations postburn-in. Multiple runs ($n = 20$) were conducted for a range of population cluster (K) values (1–12) and summarized using Structure Harvester v0.56.4 (Earl 2009). Likelihood plots were used to examine variance in runs, and using the empirical methods of Evanno *et al.* (2005), the true number of populations (K) was determined by a spike in ΔK.

Results

Molecular data

Pertaining to the ingroup, the final alignment for *ND2* contains 1056 base pairs (200 variable sites, 154 parsimony informative), *KIF24* contains 554 base pairs (24 variable sites, 14 parsimony informative), *EXPH5* contains 941 base pairs (34 variable sites, 25 parsimony informative) and *RAG-1* contains 1149 base pairs (61 variable sites, 36 parsimony informative). The percentage of parsimony informative characters to total characters for each gene is as follows: *EXPH5*, 2.6%; *KIF24*, 2.5%; *RAG-1*, 3.1%; and *ND2*, 14.6%.

Network analyses

The three nuclear allele networks show various degrees of allele sharing between the Central and Southern regions, whereas the Northern alleles are typically separated from the other two regions by several mutational steps (Fig. 3c). In all three networks, the outgroup,

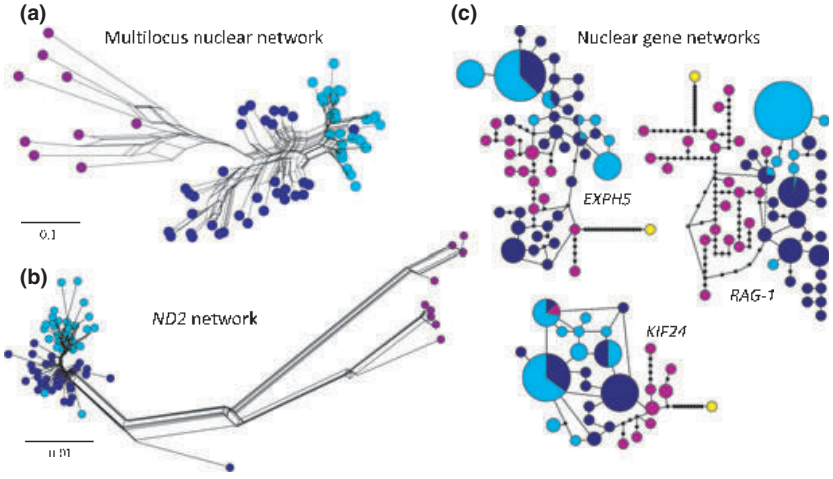

Fig. 3 Multilocus nuclear network showing overall genetic distance among individuals (a), mtDNA network showing genetic distance between individuals for *ND2* (b) and nuclear allele networks (c). The multilocus nuclear and *ND2* networks were visualized using the NeighborNet algorithm, whereas individual nuclear allele networks are based on statistical parsimony with a 95% connection significance. Colours correspond to geographic sampling regions: purple, Northern; dark blue, Central; light blue, Southern. Yellow circles are outgroup haplotypes of *Trachylepis variegata*. Scale bars reflect uncorrected pairwise differences.

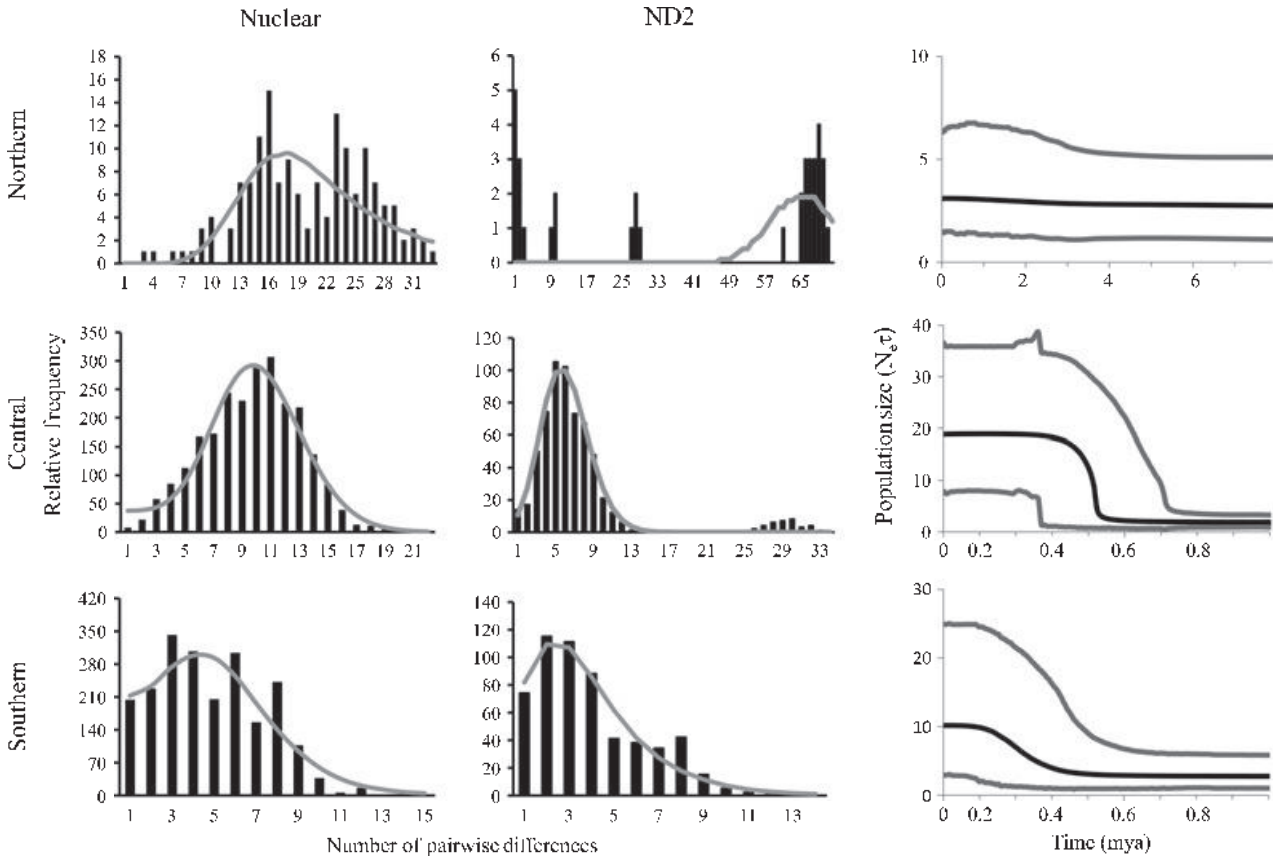

Fig. 4 Mismatch distributions and extended Bayesian skyline plots (EBSPs) for the Northern, Central and Southern regions. In the mismatch distributions, black columns represent the observed frequency of pairwise differences, whereas grey lines show an expected distribution simulated under the sudden population expansion model. The EBSPs show the estimated population size through time, expressed in millions of years. The black lines represent the median estimate of population size measured as the product of effective population size (N_e) and generation time (τ), and grey lines denote upper and lower 95% posterior intervals.

Trachylepis variegata, is most closely related to haplotypes from the Northern region, identifying these as the ancestral alleles of this species (Fig. 3c). Results from the distance networks are congruent with the parsimony networks, as Northern alleles are strongly separated from other regions and there is less differentiation between the Central and Southern regions with some allele sharing (results not shown). In the mitochondrial distance network, the Northern samples are distinctly separated by large genetic distances from the Central and Southern samples (Fig. 3b). The Central and Southern samples tend to form their own clusters, although minor allele sharing is present and the genetic distance between these clusters is small. The multilocus nuclear network depicting overall nuclear genetic distances between individuals supports a clear separation between all three geographic regions (Fig. 3a). In this network, individuals in the Northern region have the greatest genetic distances within any region or between regions, similar to the mitochondrial network.

Historical demography and molecular diversity

For the EBSPs of the Northern region, the stepwise population model with an uncorrelated lognormal clock outperformed other models ($\log_{10}$ BF ranging from 5.28 to 31.27). The stepwise population model with a strict clock was chosen for the Central region ($\log_{10}$ BF ranging from 44.64 to 70.99), and the linear population model with an uncorrelated lognormal clock was chosen for the Southern region ($\log_{10}$ BF ranging from 18.73 to 54.40). The median estimates of historical population size reveal different scenarios for each respective region (Fig. 4). The estimated population size (measured as the product of effective population size, N_e, and generation time, τ) for the Northern region is relatively stable over the last 8 million years, whereas the Central and Southern regions have experienced pronounced population expansion events. While we do not place heavy emphasis on specific dates because of calibration uncertainties, the relative timings of these

Table 2 The nucleotide diversity (π), average number of within-population pairwise differences (k), Tajima's D and Fu's Fs value for each molecular data set in the three geographic sampling areas

Population	Gene	π	k	SSD	Raggedness index	Tajima's D	Fs value
Northern	*EXPH5*	0.0056	5.22	**0.0122**	**0.0401**	−0.2120	**−4.3725**
	KIF24	0.0069	3.70	**0.0071**	**0.0354**	−0.5753	−0.4892
	RAG-1	0.0093	10.71	**0.0052**	**0.0087**	−0.5933	**−13.9534**
	Combined nuclear	0.0073	19.09	**0.0097**	**0.0147**	−0.3143	**−6.3000**
	ND2	0.0429	40.94	**0.0508**	**0.0448**	1.6593	−0.2170
Central	*EXPH5*	0.0048	4.51	**0.0034**	**0.0077**	0.1082	**−15.3681**
	KIF24	0.0024	1.30	0.0112	0.1087	−0.2278	**−10.7099**
	RAG-1	0.0025	2.85	**0.0016**	**0.0154**	−1.0092	**−16.0069**
	Combined nuclear	0.0033	8.68	**0.0017**	**0.0059**	−0.4244	**−24.7391**
	ND2	0.0071	7.10	**0.0018**	**0.0123**	**−2.2639**	**−25.0325**
Southern	*EXPH5*	0.0025	2.33	**0.0418**	**0.5340**	**2.0390**	**−6.9999**
	KIF24	0.0020	1.48	**0.0286**	**0.1217**	−0.2673	**−12.8555**
	RAG-1	0.0003	0.34	**0.0097**	**0.6187**	**−1.9079**	**−5.9749**
	Combined nuclear	0.0015	3.82	**0.0063**	**0.0192**	−0.1286	**−25.9950**
	ND2	0.0045	4.01	0.0034	**0.0214**	**−2.1984**	**−25.9439**

Significant values for Tajima's D and Fu's Fs are in bold and were assessed at $P < 0.05$. The sum of squared deviation (SSD) and raggedness index (RI) values for computed mismatch distributions are also given. Nonsignificant SSD and RI values are bolded ($P > 0.05$) and indicate failure to reject the null hypothesis of a sudden population expansion.

expansion events differ slightly between the Central region (390 000–740 000 years BP) and Southern region (330 000–670 000 years BP), with the expansion event of the Southern region being most recent. The estimated population size for the Central region is much larger than that of the Northern and Southern regions, which are more comparable in size estimates.

Mismatch analyses of the nuclear and mitochondrial data reveal results similar to those of the EBSPs (Fig. 4). In both data sets, the Central and Southern regions display unimodal distributions that do not differ significantly from the simulated expansion model (Table 2). The nuclear mismatch distribution of the Northern region shows a bimodal distribution but does not allow rejection of the null hypothesis of population expansion. In contrast, the mitochondrial mismatch distribution of the Northern region is multimodal and significantly different from the model of expansion, suggesting historical demographic stability. The overall results from Tajima's D and Fu's Fs value are concordant with the EBSP analyses, although the stochastic nature of individual gene histories is apparent (Table 2). The demographic size of the Northern region appears to have been relatively stable according to Tajima's D, although population expansion is inferred from two nuclear genes using Fu's Fs value. The Central and Southern regions test positive for recent expansion events in all genes based on Fu's Fs; however, the results for Tajima's D vary across genes in both regions. Based on nucleotide diversity and within-population pairwise differences across all genes, the Northern region contains the greatest genetic diversity in this species, while the Southern region is the area of lowest genetic diversity (Table 2). All pairwise population estimates of F_{ST} between regions were significant but varied between the nuclear and mitochondrial data. The fixation indices between regions based on nuclear and mitochondrial data, respectively, are as follows: Northern and Central region, $F_{ST} = 0.36$, 0.74; Northern and Southern region, $F_{ST} = 0.59$, 0.78; Central and Southern region, $F_{ST} = 0.40$, 0.25.

The hierarchical AMOVA analysis strongly supported a two-group model for the mitochondrial data, with the Northern region as one group and a combined group consisting of the Central and Southern regions [N vs. (CS) model] (Table 3). In this model, 78.99% of the total genetic variance is explained by differences among groups ($\phi_{CT} = 0.790$), 15.40% of the variance is explained by differences between populations within the same group ($\phi_{SC} = 0.733$) and 5.61% of the variance is attributed to differences within populations ($\phi_{ST} = 0.408$). For the nuclear data set, the percentage of variation and fixation indices among groups is nearly identical between the three-group model and the N vs. (CS) model (40.81%, $\phi_{CT} = 0.408$; 40.39%, $\phi_{CT} = 0.404$, respectively).

Population clustering

Based on likelihood plots and inspection for a peak in ΔK (Evanno *et al.* 2005), the Bayesian clustering analysis most strongly supports the presence of three populations. At $K = 3$, all except four samples are assigned to a particular population with a posterior probability

Table 3 The results of the hierarchical AMOVA analysis of the combined nuclear data and of *ND2*

	Combined nuclear data				ND2			
Model	Variation source	d.f.	Percentage of variation	Fixation indices	Variation source	d.f.	Percentage of variation	Fixation indices
3 populations	Among groups	2	40.81	ϕ_{CT} = 0.408	Among groups	2	60.19	ϕ_{CT} = 0.602
	Among populations within groups	52	20.93	ϕ_{SC} = 0.354	Among populations within groups	56	28.33	ϕ_{SC} = 0.712
	Within populations	99	38.26	ϕ_{ST} = 0.617	Within populations	20	11.48	ϕ_{ST} = 0.885
(NC) vs. S	Among groups	1	32.25	ϕ_{CT} = 0.323	Among groups	1	15.69	ϕ_{CT} = 0.157
	Among populations within groups	53	29.57	ϕ_{SC} = 0.436	Among populations within groups	57	70.47	ϕ_{SC} = 0.836
	Within populations	99	38.18	ϕ_{ST} = 0.618	Within populations	20	13.85	ϕ_{ST} = 0.157
N vs. (CS)	Among groups	1	40.39	ϕ_{CT} = 0.404	Among groups	1	78.99	ϕ_{CT} = 0.790
	Among populations within groups	53	28.61	ϕ_{SC} = 0.480	Among populations within groups	57	15.40	ϕ_{SC} = 0.733
	Within populations	99	31.00	ϕ_{ST} = 0.690	Within populations	20	5.61	ϕ_{ST} = 0.944

Three models were tested, including a three-population model (Northern, Central, Southern) and two different combined population models ((Northern and Central) vs. Southern; combined (Central and Southern) vs. Northern) to see which model maximized ϕ_{CT}, the fixation index among groups. Based on this statistic, the best-fit model for the nuclear data is the three-population model, whereas the two-population model of (Central and Southern) vs. Northern is chosen for the *ND2* data set. All ϕ-statistics significant at $P < 0.05$ are bolded.

greater than 0.80 (Fig. 5). The geographic distributions of the three populations inferred are discrete and allopatric and correspond to the three main geographic sampling regions described. A clear break is present between the Northern and Central regions, and a second break is apparent in the Knersvlakte region between the Central and Southern regions (Fig. 5). There are two samples in the Central region that show the genetic signature of samples belonging to the Southern region. When two populations are inferred, the results are not geographically concordant, as each putative population contains samples scattered across all three geographic regions.

Discussion

Our analyses have revealed a complex phylogeographic history for *Trachylepis sulcata*, with different demographic processes affecting each of the three geographic regions across the range of this species. The Northern region contains the greatest nucleotide diversity and average number of within-population pairwise differences across all genes sequenced, a finding that is characteristic of large refugial populations with long evolutionary histories and relatively little demographic fluctuation. The demographic stability of the Northern region is further supported by mismatch analyses, which exhibit multimodal patterns deviating from unimodal distributions characteristic of population expansions. Additionally, the EBSP constructed for the Northern region shows little demographic fluctuation occurring over the last 8 million years. Southern Africa was characterized by intense arid conditions during the Cretaceous period, which persisted until the Miocene or Pliocene (Tyson 1986), during which shifting climatic conditions associated with glacial cycles in the Tertiary produced vegetation mesic in composition (Van Zinderen Bakker & Mercer 1986; Lancaster 1989; Coetzee 1993). It seems that before this transition to favourable habitat, *T. sulcata* was primarily restricted to the Northern region of its current range. The nuclear parsimony networks demonstrate alleles from the Northern region are the ancestral alleles in this species, providing further support for this hypothesis. Patterns occurring in the Central and Southern regions are more typical of populations with a small effective population size that have undergone demographic expansion. Compared to the Northern region, both of these regions exhibit lower levels of genetic diversity and within-population pairwise differences, but show evidence of significant range expansion according to Fu's *Fs*, mismatch analyses and the EBSPs generated.

The levels of genetic variation across the Northern, Central, and Southern regions differ between the mito-

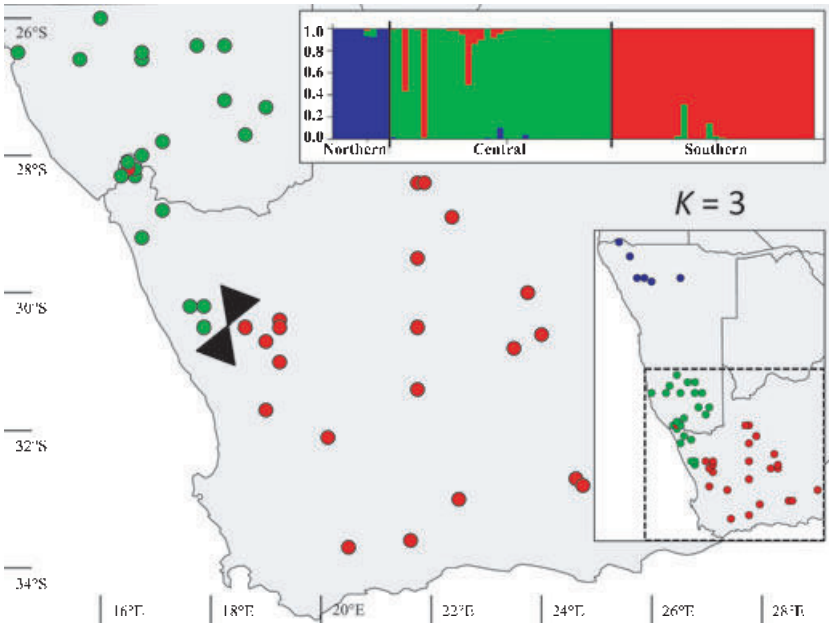

Fig. 5 The contact zone surrounding the Knersvakte region (black hourglass) based on the population clustering analysis. Circles represent sampling localities, and coloration is based on the results of the bar plot, which shows the population assignment of 76 samples into $K = 3$ populations. Population one consists of samples from Northern Namibia (Northern region), population two is made up of samples from Southern Namibia and the Northern Cape west of the Knersvlakte (Central region) and population three consists of samples from the Northern Cape east of the Knersvlakte, the Western Cape and the Eastern Cape (Southern region).

chondrial and nuclear data sets. Nuclear genetic diversity is high in both the Northern and Central regions and low in the Southern region, which explains the similar AMOVA results found for both the three-group model and the N vs. (CS) model (Table 3). In contrast, mtDNA variation is very low in both the Central and Southern regions, and most of the genetic variation occurs between the Northern region and these two regions [N vs. (CS) model]. These overall genetic diversity patterns are somewhat captured in the distance networks generated for each data set (Fig. 3a, b).

While patterns in genetic variability are useful for characterizing each geographic region, it is difficult to assess genetic connectivity between these regions using these methods. The population clustering analysis is more appropriate for this type of inference, as allele frequencies from multiple independent loci are used to detect populations in Hardy–Weinberg equilibrium. The population clustering analysis performed supports the presence of three populations corresponding to the Northern, Central and Southern sampling regions. These results are also supported by nuclear F_{ST} values, which are significant across all sampling region comparisons. We therefore recognize the presence of three genetically distinct populations.

The combined results from our analyses show important differences between the mitochondrial and nuclear data. Both nuclear and mitochondrial data sets detect a genetic break between the Northern and Central regions, yet only the nuclear markers detect the recent break between the Central and Southern regions. The lack of strong mitochondrial differentiation between the Central and Southern regions may be the result of introgression resulting from selection or drift (Ballard & Whitlock 2004). The results of Tajima's *D* and Fu's *Fs* for the mtDNA marker *ND2* suggest a deviation from neutrality or recent expansion in the Central and Southern regions. The MK test did not reveal significant differences in synonymous and nonsynonymous changes between the Northern region and Central and Southern regions ($G = 0.174$, $P = 0.6973$), suggesting this marker is not deviating from neutrality and that expansion or drift may be responsible for the patterns observed.

The apparent lack of genetic connectivity between the Northern and Central regions across Namibia is somewhat unexpected, as many squamate species display a continuous distribution pattern along the coastline (Branch 1998). As a majority of the coastline of Namibia consists of continuous Nama Karoo (sparse scrubland) habitat, major species breaks and subspecies range limits in the herpetofauna of Namibia are typically longitudinal and occur further inland, where the habitat type changes to arid savannah (Branch 1998). Sampling in the Northern region falls within both habitat types, and

climate is therefore unlikely to explain the latitudinal genetic break observed. There are no clear topological barriers present in central Namibia, and many inland squamate species show continuous distributions across this zone. Further sampling in central Namibia may allow the specific location of the mitochondrial and nuclear breaks to be detected and help explain the apparent lack of gene flow in this area. In Northern Namibia and southern Angola, desert, semidesert, and arid savannah habitats merge to create a landscape that is a contact zone for many species complexes associated with these habitats. Northern Namibia is a zone of very high genetic diversity in *T. sulcata*, is close to the contact zone of *T. s. sulcata* and *T. s. ansorgii* and is also an area that warrants additional studies of sympatrically distributed taxa.

Both the Orange River and the Knersvlakte have been proposed as biogeographic barriers affecting the fauna of southern Africa (Branch & Bauer 1995; Matthee & Robinson 1996; Lamb & Bauer 2000; Matthee & Flemming 2002; Smit *et al.* 2007). We find no evidence of genetic differentiation in *T. sulcata* corresponding to the Orange River, but our results do support the presence of a significant genetic break across the Knersvlakte region. The Knersvlakte region has been found to be an important biogeographic barrier in other rupicolous species, such as the red rock rabbit (Matthee & Robinson 1996), the rock agama (Matthee & Flemming 2002; Swart *et al.* 2009), the speckled padloper (Daniels *et al.* 2010) and the Cape rock elephant shrew (Smit *et al.* 2007). The genetic breaks in these species were detected using mtDNA; however, our analyses of mtDNA in this study are inconsistent with this pattern, owing to stochastic processes or introgression. Rather, differences in allele frequencies across three nuclear loci revealed the presence of two distinct populations divided by the Knersvlakte.

The concordant genetic break across the Knersvlakte region in *T. sulcata* and four other rupicolous species suggests that dispersal across the Knersvlakte is limited, although the levels of genetic exchange occurring between respective populations have never been explicitly investigated and sampling in previous studies is not as fine-scale as ours. The formation of the Knersvlakte region is associated with the uplift of the great western escarpment during the Miocene, approximately 18 mya (Moon & Dardis 1988). Estimates of the divergence between populations of *A. atra* divided by the Knersvlakte range from 715 000 years BP to 2.2–4.4 mya using allozyme and mtDNA data, respectively (Matthee & Flemming 2002), whereas the estimate for the divergence between the Cape rock elephant shrew populations is 2.41 mya based on mtDNA data (Smit *et al.* 2007). The estimate of population expansion in *T. sulcata* in the Southern region based on the EBSP of all four markers with a mitochondrial calibration of 0.47% change per lineage per million years indicates significant expansion occurred in the mid-Pleistocene (approximately 330 000–670 000 years BP), making it the most recent arrival of the taxa studied.

The timing of the genetic breaks of all taxa studied suggests dispersal across the Knersvlakte region took place long after its uplift was completed. The contact zones found around the Knersvlakte for the other species differ geographically from the contact zone described for *T. sulcata* populations. The contact zone present in *T. sulcata* is an east to west break, rather than a north to south break (Fig. 5). These results contrast sharply with the contact zones of *A. atra*, *P. rupestris* and *E. edwardii*, which are characterized by a latitudinal break at the Knersvlakte that extends eastward across northern South Africa (Matthee & Robinson 1996; Matthee & Flemming 2002; Smit *et al.* 2007). This difference exhibited by *T. sulcata* can be explained by a unique southward colonization of this area followed by an eastern expansion and is the first explicitly investigated case of a southward invasion of South Africa.

Acknowledgements

Funding for this project was provided by a National Science Foundation grant (DEB 0515909) and Villanova University. We thank Bill Branch, Marius Burger, Johan Marais, Richard Boycott and Krystal Tolley for tissue samples. Ross Sadlier, Johan Marais and Stuart Love Nielsen provided assistance in the field. We also thank the authorities in the Republic of Namibia and the Northern, Western and Eastern Cape provinces of the Republic of South Africa permitting the collection and export of samples used in this study.

References

Ballard JWO, Whitlock MC (2004) The incomplete natural history of mitochondria. *Molecular Ecology*, **13**, 729–744.

Bauer AM (1999) Evolutionary scenarios in the *Pachydactylus* Group geckos of southern Africa: new hypotheses. *African Journal of Herpetology*, **48**, 53–62.

Bauer AM, Branch WR (2001) The herpetofauna of the Richtersveld National Park and the adjacent northern Richtersveld, northern Cape Province, Republic of South Africa. *Herpetological Natural History*, **8**, 111–160.

Bauer AM, Branch WR, Haacke WD (1993) The herpetofauna of the Kamanjab area and adjacent Damaraland, Namibia. *Madoqua*, **18**, 117–145.

Beheregaray LB (2008) Twenty years of phylogeography: the state of the field and the challenges for the Southern Hemisphere. *Molecular Ecology*, **17**, 3754–3774.

Branch B (1998) *Field Guide to Snakes and Other Reptiles of Southern Africa*, 3rd edn. Ralph Curtis Books Publishing, Sanibel Island.

Branch WR, Bauer AM (1995) Herpetofauna of the Little Karoo, Western Cape, South Africa with notes on life history and taxonomy. *Herpetological Natural History*, **3**, 47–89.

Branch WR, Bauer AM, Good DA (1995) Species limits in the *Phyllodactylus lineatus* complex (Reptilia: Gekkonidae), with the elevation of two taxa to specific status and the description of two new species. *Journal of the Herpetological Association of Africa*, **44**, 33–54.

Bryant D, Moulton V (2004) Neighbor-Net: an agglomerative method for the construction of phylogenetic networks. *Molecular Biology and Evolution*, **21**, 255–265.

Chase BM, Meadows ME (2007) Late Quaternary dynamics of southern Africa's winter rainfall zone. *Earth-Science Reviews*, **84**, 103–138.

Clement M, Posada D, Crandall KA (2000) TCS: a computer program to estimate gene genealogies. *Molecular Ecology*, **9**, 1657–1659.

Coetzee JA (1993) African flora since the Terminal Jurassic. In: *Biological Relationships between Africa and South America* (ed. Goldblatt P). pp. 37–61, Yale University Press, New Haven.

Cowling RM, Proches S, Partridge TC (2009) Explaining the uniqueness of the Cape flora: incorporating geomorphic evolution as a factor for explaining its diversification. *Molecular Phylogenetics and Evolution*, **51**, 64–74.

Daniels SR, Mouton P, Du Toit DA (2004) Molecular data suggest that melanistic ectotherms at the south-western tip of Africa are the products of Miocene climatic events: evidence from cordylid lizards. *Journal of Zoology*, **263**, 373–383.

Daniels SR, Hofmeyr MD, Henen BT, Crandall KA (2007) Living with the genetic signature of Miocene induced change: evidence from the phylogeographic structure of the endemic angulate tortoise *Chersina angulata*. *Molecular Phylogenetics and Evolution*, **45**, 915–926.

Daniels SR, Hofmeyr MD, Henen BT, Baard EHW (2010) Systematics and phylogeography of a threatened tortoise, the speckled padloper. *Animal Conservation*, **13**, 237–246.

Drummond AJ, Rambaut A (2007) BEAST: Bayesian evolutionary analysis by sampling trees. *BMC Evolutionary Biology*, **7**, 214–222.

Drummond AJ, Rambaut A, Shapiro B, Pybus OG (2005) Bayesian coalescent inference of past population dynamics from molecular sequences. *Molecular Biology and Evolution*, **22**, 1185–1192.

Drummond A, Ashton B, Cheung M *et al.* (2009) Geneious v4.6. Available from http://www.geneious.com/.

Earl DA (2009) Structure Harvester v0.3. Available from http://users.soe.ucsc.edu/~dearl/software/struct_harvest/.

Evanno G, Regnaut S, Goudet J (2005) Detecting the number of clusters of individuals using the software STRUCTURE: a simulation study. *Molecular Ecology*, **14**, 2611–2620.

Excoffier LGL, Schneider S (2005) Arlequin ver. 3.0: an integrated software package for population genetics data analysis. *Evolutionary Bioinformatics*, **1**, 47–50.

Excoffier L, Smouse PE, Quattro JM (1992) Analysis of molecular variance inferred from metric distances among DNA haplotypes application to human mitochondrial DNA restriction data. *Genetics*, **131**, 479–491.

Fu YX (1997) Statistical tests of neutrality of mutations against population growth, hitchhiking and background selection. *Genetics*, **147**, 915–925.

Heled J, Drummond A (2008) Bayesian inference of population size history from multiple loci. *BMC Evolutionary Biology*, **8**, 289.

Huson DH, Bryant D (2006) Application of phylogenetic networks in evolutionary studies. *Molecular Biology and Evolution*, **23**, 254–267.

Joly S, Bruneau A (2006) Incorporating allelic variation for reconstructing the evolutionary history of organisms from multiple genes: an example from *Rosa* in North America. *Systematic Biology*, **55**, 623–636.

Kass RE, Raftery AE (1995) Bayes factors. *Journal of the American Statistical Association*, **90**, 773–795.

Lamb T, Bauer AM (2000) Relationships of the *Pachydactylus rugosus* group of geckos (Reptilia : Squamata : Gekkonidae). *African Zoology*, **35**, 55–67.

Lancaster N (1989) Late Quaternary paleoenvironments in the southwestern Kalahari. *Paleogeography, Paleoclimate, Paleoecology*, **70**, 367–376.

Laurent RL (1964) Reptiles et amphibiens de l'Angola (troisième contribution). *Publicações Culturais da Companhia de Diamantes de Angola*, **67**, 1–165.

Lesia MGA, Hofmeyr MD, D'Amato ME (2003) Genetic variation in three *Chersina angulata* (angulate tortoise) populations along the west coast of South Africa. *African Zoology*, **38**, 109–117.

Librado P, Rozas J (2009) DnaSP v5: a software for comprehensive analysis of DNA polymorphism data. *Bioinformatics (Oxford)*, **25**, 1451–1452.

Macey JR, Larson A, Ananjeva NB, Papenfuss TJ (1997) Evolutionary shifts in three major structural features of the mitochondrial genome among iguanian lizards. *Journal of Molecular Evolution*, **44**, 660–674.

Macey JR, Schulte II JA, Ananjeva NB *et al.* (1998) Phylogenetic relationships among Agamid lizards of the *Laudakia caucasia* species group: testing hypotheses of biogeographic fragmentation and an area cladogram for the Iranian Plateau. *Molecular Phylogenetics and Evolution*, **10**, 118–131.

Makokha JS (2006) Molecular phylogenetics and phylogeography of sand lizards, *Pedioplanis* (Sauria: Lacertidae) in southern Africa. Unpublished Ph.D. dissertation. University of Stellenbosch, Stellenbosch.

Makokha JS, Bauer AM, Mayer W, Matthee CA (2007) Nuclear and mtDNA-based phylogeny of southern African sand lizards, *Pedioplanis* (Sauria: Lacertidae). *Molecular Phylogenetics and Evolution*, **44**, 622–633.

Matthee CA, Flemming AF (2002) Population fragmentation in the southern rock agama, *Agama atra*: more evidence for vicariance in Southern Africa. *Molecular Ecology*, **11**, 465–471.

Matthee CA, Robinson TJ (1996) Mitochondrial DNA differentiation among geographical populations of *Pronolagus rupestris*, Smith's red rock rabbit (Mammalia: Lagomorpha). *Heredity*, **76**, 514–523.

McDonald JH, Kreitman M (1991) Adaptive protein evolution at the *Adh* locus in *Drosophila*. *Nature*, **351**, 652–654.

Mertens R (1955) Die Amphibien und Reptilien Südwestafrikas, aus den Ergebnissen einer im Jahre 1952 ausgeführten Rei- se. *Abhandlungen der Senckenbergischen naturforschenden Gesellschaft*, **490**, 1–172.

Mertens R (1971) Die Herpetofauna Südwest-Afrikas. *Abhandlungen der Senckenbergischen naturforschenden Gesellschaft*, **529**, 1–110.

Moon BP, Dardis GF (1988) *The Geomorphology of Southern Africa*. CTP Book Printers, Cape Town, South Africa.

Newton MA, Raftery AE, Davison AC *et al.* (1994) Approximate Bayesian-Inference with the weighted likelihood bootstrap. *Journal of the Royal Statistical Society Series B-Methodological*, **56**, 3–48.

Portik DM, Bauer AM, Jackman TR (2010) The phylogenetic affinities of *Trachylepis sulcata nigra* and the intraspecific evolution of coastal melanism in the western rock skink. *African Zoology*, **45**, 147–159.

Posada D (2008) jModelTest: Phylogenetic Model Averaging. *Molecular Biology and Evolution*, **25**, 1253–1256.

Pritchard JK, Stephens M, Donnelly P (2000) Inference of population structure using multilocus genotype data. *Genetics*, **155**, 945–959.

Rambaut A, Drummond AJ (2009) Tracer v1.5.0. Available from http://beast.bio.ed.ac.uk/.

Rogers AR, Harpending H (1992) Population growth makes waves in the distribution of pairwise genetic differences. *Molecular Biology and Evolution*, **9**, 552–569.

Scheet P, Stephens M (2006) A fast and flexible statistical model for large-scale population genotype data: applications to inferring missing genotypes and haplotypic phase. *American Journal of Human Genetics*, **78**, 629–644.

Slatkin M, Hudson RR (1991) Pairwise comparisons of mitochondrial DNA sequences in stable and exponentially growing populations. *Genetics*, **129**, 555–562.

Smit HA, Robinson TJ, van Vuuren BJ (2007) Coalescence methods reveal the impact of vicariance on the spatial genetic structure of *Elephantulus edwardii* (Afrotheria, Macroscelidae). *Molecular Ecology*, **16**, 2680–2692.

Stephens M, Smith NJ, Donnelly P (2001) A new statistical method for haplotype reconstruction from population data. *American Journal of Human Genetics*, **68**, 978–989.

Suchard MA, Weiss RE, Sinsheimer JS (2001) Bayesian selection of continuous-time Markov chain evolutionary models. *Molecular Biology and Evolution*, **18**, 1001–1013.

Swart BL, Tolley KA, Matthee CA (2009) Climate change drives speciation in the southern rock agama (*Agama atra*) in the Cape Floristic Region, South Africa. *Journal of Biogeography*, **36**, 78–87.

Tajima F (1989) Statistical method for testing the neutral mutation hypothesis by DNA polymorphism. *Genetics*, **123**, 585–595.

Tolley KA, Tilbury CR, Branch WR, Matthee CA (2004) Phylogenetics of the southern African dwarf chameleons, *Bradypodion* (Squamata: Chamaeleonidae). *Molecular Phylogenetics and Evolution*, **30**, 354–365.

Tolley KA, Burger M, Turner AA, Matthee CA (2006) Biogeographic patterns and phylogeography of dwarf chameleons (*Bradypodion*) in an African biodiversity hotspot. *Molecular Ecology*, **15**, 781–793.

Tolley KA, Chase BM, Forest F (2008) Speciation and radiations track climate transitions since the Miocene Climatic Optimum: a case study of southern African chameleons. *Journal of Biogeography*, **35**, 1402–1414.

Tolley KA, Makokha JS, Houniet DT, Swart BL, Matthee CA (2009) The potential for predicted climate shifts to impact genetic landscapes of lizards in the South African Cape Floristic Region. *Molecular Phylogenetics and Evolution*, **51**, 120–130.

Townsend TM, Larson A, Louis E, Macey JR (2004) Molecular phylogenetics of Squamata: the position of snakes, amphisbaenians, and dibamids, and the root of the squamate tree. *Systematic Biology*, **53**, 735–757.

Tyson PD (1986) *Climatic Change and Variability in Southern Africa*. Oxford University Press, Cape Town.

Van der Niet T, Johnson SD (2009) Patterns of plant speciation in the Cape floristic region. *Molecular Phylogenetics and Evolution*, **51**, 85–93.

Van Zinderen Bakker EM, Mercer JH (1986) Major late Cainozoic climatic events and paleoenvironmental changes in Africa viewed in a world wide context. *Paleogeography, Paleoclimate, Paleoecology*, **56**, 217–235.

Verboom GA, Archibald JK, Bakker FT *et al.* (2009a) Origin and diversification of the Greater Cape flora: ancient species repository, hot-bed of recent radiation, or both? *Molecular Phylogenetics and Evolution*, **51**, 44–53.

Verboom GA, Dreyer LL, Savolainen V (2009b) Understanding the origins and evolution of the world's biodiversity hotspots: the biota of the African 'Cape Floristic Region' as a case study. *Molecular Phylogenetics and Evolution*, **51**, 1–4.

D.M.P. is interested in patterns of phylogeography, speciation, and character development in African amphibians and reptiles. This work represents part of his Master's research conducted at Villanova University, and he is currently a PhD candidate at the University of California, Berkeley. A.M.B. has published extensively on the topics of herpetology, biogeography, systematics, vertebrate morphology, and the history of biology. T.R.J.'s research focuses on reconstructing the history of populations representing different stages of speciation as well as using DNA sequence data in combination with other data to provide historical frameworks for examining evolutionary processes

---

Appendix

ID numbers, species identification and geographic location of specimens sequenced for this study. AMB, Aaron M. Bauer field number; AMS, Australian Museum, Sydney; CAS, California Academy of Sciences; KTH, Krystal Tolley field number, SANBI, South African National Biodiversity Institute, Kirstenbosch; LSUMZ, Louisiana Museum of Natural History; MB, MBUR, Marius Burger field number; MCZ, Museum of Comparative Zoology, Harvard University; NMB, National Museum Bloemfontein; NMN, National Museum of Namibia; PEM, Bayworld (Port Elizabeth Museum); SAM, South African Museum, Cape Town. Museum abbreviations without indication of specimen registration numbers pending accessions.

Trachylepis species	Field number	Museum number	Locality	Latitude	Longitude
sulcata	AMB 4288	CAS 199999	Hwy N7, 6 km S of Garies	30°36′47″S	18°01′15″E
sulcata	AMB 4291	PEM 11914	South Africa, Steinkopf	29°20′16″S	17°47′31″E
sulcata	AMB 4596	CAS 200043	South Africa, Northern Cape, Richtersveld National Park, rd to Wallekraal Mines	28°20′10″S	16°54′34″E
sulcata	AMB 4620	PEM 11875	South Africa, Northern Cape, Richtersveld National Park	28°20′31″S	16°58′36″E
sulcata	AMB 4693	LSUMZ 57296	South Africa, Northern Cape, Richtersveld National Park	28°09′48″S	17°01′10″E
sulcata	AMB 4766	PEM 11868	South Africa, Northern Cape, Richtersveld National Park	28°12′12″S	17°06′37″E
sulcata	AMB 4767	PEM 12413	South Africa, Northern Cape, Richtersveld National Park	28°12′12″S	17°06′37″E
sulcata	AMB 4782	LSUMZ 57297	South Africa, Northern Cape, 2.7 km from Khuboes on Swartbank Rd	28°25′31″S	17°00′04″E
sulcata	AMB 4790	LSUMZ 57298	South Africa, Northern Cape, Richtersveld National Park; 1.8 km up Nicodemes from jct w/Hottentotsparadys overlook	28°19′30″S	16°58′04″E
sulcata	AMB 6837	NMN	Namibia, Karasburg-Aroab Rd, 16.0 km NE Karasburg	27°52′54″S	18°47′22″E
sulcata	AMB 6838	CAS 223993	Namibia, Karasburg-Aroab Rd, 16.0 km NE Karasburg	27°52′54″S	18°47′22″E
sulcata	AMB 6839	NMN	Namibia, Karasburg-Aroab Rd, 16.0 km NE Karasburg	27°52′54″S	18°47′22″E
sulcata	AMB 6895	AMS	Namibia, along C40 W of Kamanjab	19°41′00″S	14°19′10″E
sulcata	AMB 6971	AMS	Namibia, Kunene Region, Kaoko Otavi-Opuwo rd, 4.2 km E of Sesfontein Rd jct	18°12′45″S	13°48′00″E
sulcata	AMB 6972	NMN	Namibia, Kunene Region, Kaoko Otavi-Opuwo rd, 4.2 km E of Sesfontein Rd jct	18°12′45″S	13°48′00″E
sulcata	AMB 6979	CAS 223994	Namibia, Kunene Region, Kaoko Otavi-Opuwo rd, 4.2 km E of Sesfontein Rd jct	18°12′45″S	13°48′00″E
sulcata	AMB 6981	CAS 223996	Namibia, Kunene Region, Kaoko Otavi-Opuwo rd, 4.2 km E of Sesfontein Rd jct	18°12′45″S	13°48′00″E
sulcata	AMB 6987	CAS 223979	Namibia, Kunene Region, Kaoko Otavi-Opuwo rd, 4.2 km E of Sesfontein Rd jct	18°12′45″S	13°48′00″E
sulcata	AMB 7115	NMN	Namibia, 3.8 km E Keetmanshoop	26°37′10″S	18°07′26″E
sulcata	AMB 8171	MCZ R-184394	South Africa, Eastern Cape, Farm Newstead	32°06′04″S	26°15′19″E
sulcata	AMB 8172	MCZ R-184395	South Africa, Eastern Cape, Farm Newstead	32°06′04″S	26°15′19″E
sulcata	AMB 8173	MCZ R-184396	South Africa, Eastern Cape, Farm Newstead	32°06′04″S	26°15′19″E
sulcata	AMB 8175	MCZ R-184398	South Africa, Eastern Cape, Farm Newstead	32°06′04″S	26°15′19″E
sulcata	AMB 8176	MCZ R-184399	South Africa, Eastern Cape, Farm Newstead	32°06′04″S	26°15′19″E
sulcata	JM 1106	PEM 17732	Namibia, Ai-Ais	27°54′49″S	17°29′26″E
sulcata	JM 1107	PEM 17737	Namibia, Ai-Ais	28°54′49″S	17°29′26″E
sulcata	JM 1119	PEM 17744	South Africa, Northern Cape, N of Khargams	30°21′08″S	17°53′06″E
sulcata	JM 1186	PEM 17733	South Africa, Northern Cape, Road to Bloeddrif, Richtersveld	28°22′23″S	16°49′41″E
sulcata	KTH 200	PEM	South Africa, Western Cape, Tankwa Karoo	32°16′50″S	20°06′21″E
sulcata	KTH 240	PEM	South Africa, Western Cape, Tankwa Karoo	32°16′50″S	20°06′21″E
sulcata	KTH 534	PEM	Kalahari		
sulcata	KTH 538	SAM	South Africa, Western Cape, Marloth NR, Goedgeloof, Langeberg	33°57′07″S	20°27′29″E
sulcata	Mab121	CAS 180413	South Africa, Western Cape, Little Karoo, Rooiberg	33°44′11″S	21°36′21″E
sulcata	MB 20603	PEM 17045	South Africa, Northern Cape, Farm Donkiedam, (NW of Loeriesfontein), at Nek se Kamp	30°55′02″S	19°03′37″E
sulcata	MB 20604	PEM 17054	South Africa, Northern Cape, Farm Donkiedam, (NW of Loeriesfontein), at Nek se Kamp	31°55′02″S	19°03′37″E
sulcata	MB 20627	PEM 17053	South Africa, Northern Cape, Farm Donkiedam, (NW of Loeriesfontein), near trap 1-9	30°55′29″S	19°02′54″E
sulcata	MB 20632	PEM 17098	South Africa, Northern Cape, along road past farm Bloukrans, SW of Loeriesfontein	31°11′39″S	19°18′19″E
sulcata	MB 20644	PEM 17050	South Africa, Northern Cape, Farm Loerkop, N of Loeriesfontein	30°39′23″S	19°20′33″E
sulcata	MB 20664	PEM 17051	South Africa, Northern Cape, Farm Die Kop, N of Loeriesfontein	30°34′41″S	19°20′32″E

Trachylepis species	Field number	Museum number	Locality	Latitude	Longitude
sulcata	MB 20689	PEM 17058	South Africa, Northern Cape, Farm Kamas, E of Kliprand	30°35′28″S	18°49′20″E
sulcata	MB 20720	PEM 17052	South Africa, Northern Cape, Farm Donkiedam, NW of Loeriesfontein	30°55′29″S	19°02′54″E
sulcata	MB 20726	PEM 17060	South Africa, Northern Cape, Farm Eselsfontein (S of Grootdrink), at trap 2-3	28°36′42″S	21°42′01″E
sulcata	MB 20736	PEM 17055	South Africa, Northern Cape, Farm Eselsfontein (S of Grootdrink), at trap 2-3	29°36′42″S	21°42′01″E
sulcata	MB 20737	PEM 17057	South Africa, Northern Cape, Farm Eselsfontein (S of Grootdrink), at trap 2-3	30°36′42″S	21°42′01″E
sulcata	MB 20739	PEM 17059	South Africa, Northern Cape, Farm Eselsfontein (S of Grootdrink), at trap 2-3	31°36′42″S	21°42′01″E
sulcata	MB 20804	PEM 17014	South Africa, Northern Cape, Farm Eselsfontein Noord, S of Grootdrink	28°37′30″S	21°45′09″E
sulcata	MB 20892	PEM or NMB	South Africa, Northern Cape, Farm Boseekoebaard, SE of Groblershoop	29°02′57″S	22°15′37″E
sulcata	MB 21103	NMB R9252		30°48′53″S	23°38′36″E
sulcata	MB 21104	NMB R9253		30°46′20″S	23°40′17″E
sulcata	MB 21140	NMB R9254	South Africa, Northern Cape, E of Leebskop	30°55′53″S	23°13′54″E
sulcata	MB 21191	PEM	South Africa, Northern Cape, NE of Platkop	30°08′40″S	23°28′14″E
sulcata	MB 21235	PEM		30°08′43″S	23°28′17″E
sulcata	MB 21249	PEM		30°08′40″S	23°28′14″E
sulcata	MBUR 00577	PEM		32°50′47″S	24°25′21″E
sulcata	MBUR 00578	PEM		32°50′38″S	24°26′07″E
sulcata	MBUR 00603	PEM	South Africa, Eastern Cape, Grasberg	32°52′28″S	24°29′22″E
sulcata	MBUR 00707	PEM		33°07′30″S	22°20′18″E
sulcata	MBUR 00726	PEM	South Africa, Western Cape, W of Tierberg	33°07′24″S	22°19′59″E
sulcata	MBUR 01797	PEM	South Africa, Northern Cape, lower slopes of the Rooiberg, Garies district	30°24′37″S	18°05′47″E
sulcata	MBUR 01798	PEM	South Africa, Northern Cape, lower slopes of the Rooiberg, Garies district	30°24′37″S	18°05′47″E
sulcata	MCZ Z23125	MCZ R-185913	Namibia, Farm Otjitambi	19°51′33″S	15°11′45″E
sulcata	MCZ Z23140	MCZ R-185917	Namibia, 2 km E of Tses on Berseba rd	25°53′20″S	18°04′54″E
sulcata	MCZ Z23148	MCZ R-185918	Namibia, Brukkaros Mt, S slope	25°53′49″S	17°46′38″E
sulcata	MCZ Z37867	NMN	Namibia, Kamanjab, Kamanjab Rest Camp	19°37′47″S	14°48′56″E
sulcata	MCZ A38257	MCZ R-184343	Namibia, 1 km S of jct. D831 on C14 towards Helmeringhausen	25°24′54″S	16°47′49″E
sulcata	MCZ A38292	MCZ R-184351	Namibia, Konkiep	26°44′56″S	17°13′16″E
sulcata	MCZ A38293	NMN	Namibia, Konkiep	26°44′56″S	17°13′16″E
sulcata	MCZ A38303	NMN	Namibia, Savanna Guest Farm nr. Grünau	27°22′34″S	18°29′42″E
sulcata	MCZ A38331	NMN	Namibia, Savanna Guest Farm	27°23′10″S	18°29′30″E
sulcata	MCZ A38357	MCZ R-184374	Namibia, Savanna Guest Farm	27°22′56″S	18°28′36″E
sulcata	MCZ A38359	MCZ R-184375	Namibia, Savanna Guest Farm	27°22′56″S	18°28′36″E
sulcata	MCZ A38379	MCZ R-184386	Namibia, Savanna Guest Farm	27°22′32″S	18°29′33″E
sulcata	MCZ F38432	MCZ R-184770	South Africa, Northern Cape, Port Nolloth Rd	29°18′59″S	17°05′13″E
sulcata	MCZ F38481	MCZ R-184820	Namibia, Farm Savanna	27°22′35″S	18°29′33″E
sulcata	MCZ F38482	MCZ R-184821	Namibia, Farm Savanna	27°22′35″S	18°29′33″E
sulcata	MCZ F38521	MCZ R-184875	Namibia, Farm Uisib	19°33′06″S	17°14′11″E

Trachylepis species	Field number	Museum number	Locality	Latitude	Longitude
sulcata	MCZ F38643	MCZ R-185047	Namibia, Farm Tiras	26°08′49″S	16°34′10″E
sulcata	MCZ F38646	MCZ R-185006	Namibia, Geister Schlucht (Klein Aus Vista)	26°40′36″S	16°13′39″E
sulcata	MCZ F38675	MCZ R-185064	Namibia, 32 km W of Guruchab Pass on Rd C16 from Keetmanshoop to Aroab	26°36′18″S	18°28′42″E
sulcata	MCZ A38699	MCZ R-185113	Namibia, Farm Oas	27°29′37″S	19°13′20″E
sulcata	MCZ 38700	MCZ R-185114	Namibia, Farm Oas	27°29′37″S	19°13′20″E
sulcata	MCZ A38932	MCZ R-185901	Namibia, 58 km W Kamanjab Rest Camp on Rd. to Grootberg Pass	19°38′57″S	14°21′33″E
sulcata	MCZ A38958	MCZ R-185905	Namibia, on C43 near Okangwati	17°17′24″S	13°09′31″E
sulcata		PEM R 16724	Little Karoo		
sulcata nigra	MCZ Z23166	MCZ R-185923	Namibia, Lüderitz Bay, Agate Beach	26°36′49″S	15°10′14″E
sulcata nigra	MCZ Z23167	MCZ R-185924	Namibia, Lüderitz Bay, Agate Beach	26°36′49″S	15°10′14″E
variegata	AMB 7165	NMN	Namibia, on C34 N of Swakopmund	22°25′49″S	14°27′44″E